AGU PUBLICATIONS

Earth's Future

RESEARCH ARTICLE
10.1002/2016EF000399

Global atmospheric response to emissions from a proposed reusable space launch system

Erik J. L. Larson[1,2], Robert W. Portmann[1], Karen H. Rosenlof[1], David W. Fahey[1], John S. Daniel[1], and Martin N. Ross[3]

[1]Chemical Sciences Division, Earth Systems Research Laboratory, NOAA, Boulder, Colorado, USA, [2]Cooperative Institute for Research in Environmental Sciences, University of Colorado, Boulder, Colorado, USA, [3]The Aerospace Corporation, Los Angeles, California, USA

Key Points:
- Roughly 10^5 flights per year from hydrogen fueled reusable launch systems are necessary to significantly impact the global climate
- Water vapor emissions from 10^5 flights per year increase polar stratospheric and mesospheric cloud fractions by 20%
- NO_X emissions from ascent and reentry of 10^5 flights per year result in the loss of 0.5% of the globally averaged ozone column

Supporting Information:
- Supporting Information S1

Correspondence author:
E. J. L. Larson, erik.larson@noaa.gov

Citation:
Larson, E. J. L., R. W. Portmann, K. H. Rosenlof, D. W. Fahey, J. S. Daniel, and M. N. Ross (2017), Global atmospheric response to emissions from a proposed reusable space launch system, *Earth's Future*, *5*, 37–48, doi:10.1002/2016EF000399.

Received 1 JUL 2016
Accepted 11 NOV 2016
Accepted article online 16 NOV 2016
Published online 4 JAN 2017

Abstract Modern reusable launch vehicle technology may allow high flight rate space transportation at low cost. Emissions associated with a hydrogen fueled reusable rocket system are modeled based on the launch requirements of developing a space-based solar power system that generates present-day global electric energy demand. Flight rates from 10^4 to 10^6 per year are simulated and sustained to a quasisteady state. For the assumed rocket engine, H_2O and NO_X are the primary emission products; this also includes NO_X produced during reentry heating. For a base case of 10^5 flights per year, global stratospheric and mesospheric water vapor increase by approximately 10 and 100%, respectively. As a result, high-latitude cloudiness increases in the lower stratosphere and near the mesopause by as much as 20%. Increased water vapor also results in global effective radiative forcing of about 0.03 W/m^2. NO_X produced during reentry exceeds meteoritic production by more than an order of magnitude, and along with in situ stratospheric emissions, results in a 0.5% loss of the globally averaged ozone column, with column losses in the polar regions exceeding 2%.

1. Introduction

The expected availability of low cost, reusable launch systems and increasing demand for space services suggest that the global space transport industry will grow significantly in the coming decades. Relatively few studies of the chemical and climate effects of rocket emissions have been published that use current state-of-the-art atmospheric models to address the future growth scenarios. Rocket emissions are becoming more like aviation emissions in that the space sector exhibits consistent growth that cannot be reduced without serious economic disruption. Unlike the aviation sector, the most significant method of managing emissions is through prudent use of the various available propellants. Hydrogen (H_2) fuel and reusability are likely to play important roles in any future scheme to minimize the atmospheric impacts of rockets; therefore, it is important to understand the consequences of H_2 fuel and reentry emissions. Significant increases in space transport will be associated with proportional increases in combustion emissions. Some of the proposed propulsion systems make greater use of "clean-burning" H_2 fuel [*Li et al*., 2004; *Khan et al*., 2013], which has H_2O as the primary emission and thus avoids the effects of chlorine, alumina, and black carbon emissions associated with current conventional technology [*Ross et al*., 2009, 2010]. H_2 burning rocket engines may also reduce payload-to-space costs, which could dramatically increase the number of rocket launches.

Reaction Engines Ltd. (http://www.reactionengines.co.uk/) has proposed the Skylon vehicle, which is a reusable H_2-burning rocket [*Martin et al*., 2008]. Skylon would be considered a medium lift launch vehicle in the current space transport vernacular. There is a concept plan to use this vehicle to build a space-based solar power system. To be economically viable, the plan calls for a minimum of 10^4 launches per year for 10 years [*Martin et al*., 2008; *Henson*, 2014]. This rate would transport enough payload to space to build 3000 1-GW solar power stations as estimated by the National Security Space Office [*SBSP Study Group*, 2007] and Reaction Engines [*Martin et al*., 2008].

It is often assumed that H_2-fueled rocket engines have no impact on the global atmosphere since the only significant emission is H_2O. However, in great enough quantities the emissions from these rockets can alter the stratosphere in many ways. H_2O emissions can change stratospheric temperatures and alter the

photochemistry controlling ozone (O_3). Furthermore, rockets burning liquid H_2 and oxygen (O_2) use an H_2-rich mixture rather than a stoichiometric ratio for enhanced thrust and emit H_2 and HO_X in the plume in addition to H_2O. Enhancements in HO_X can catalytically destroy O_3 [*Crutzen*, 1969]. Superheated air in the engine and exhaust plume result in the production of NO_x, which also catalytically destroys O_3 [*Johnston*, 1971; *Ross et al*., 2009; *Lee et al*., 2010]. NO_x is also created in the mesosphere due to the heat produced during rocket reentry [*Park*, 1976]. Here we use the Whole Atmosphere Community Climate Model (WACCM) [*Marsh et al*., 2013] and the 2D National Oceanic and Atmospheric Administration/National Center for Atmospheric Research (NOCAR) model [*Portmann and Solomon*, 2007] to evaluate the potential effects of high Skylon launch rates on the climate and stratospheric O_3.

2. Calculating Emissions

Vertical profiles of NO_X, H_2, and H_2O emitted during a Skylon rocket launch and reentry are estimated based on trajectory data from Reaction Engines Ltd. [http://www.reactionengines.co.uk/tech_docs.html]. Skylon rockets have two combustion phases as they ascend through the atmosphere. The first phase is air breathing from the surface to 28.5 km. During this phase the engines act as H_2 burning jet turbines, combusting H_2 with ambient air. The main exhaust is H_2O, which can be calculated directly from the amount of H_2 fuel consumed. During the second phase from 28 to 80 km the engines run in rocket mode, burning H_2 and liquid O_2. The H_2O produced in rocket mode is calculated from the mass of fuel used assuming a 6:1 mass ratio of oxygen to hydrogen; this assumption is made to be consistent with the fact that many rockets burn hydrogen-rich fuel for greater thrust (stoichiometric ratio for combustion is 8:1) [*Colasurdo et al*., 1998]. Although the excess H_2 likely oxidizes into H_2O in the plume due to high temperatures, H_2 emissions are also considered in our simulations as a bounding condition. The bounding cases assume either all or none of the excess H_2 is oxidized to H_2O in the plume. As discussed in the results, the intermediate combustion products HO_X and H_2O_2 were tested with the NOCAR model and found not to be important contributors to O_3 destruction. Thus they are not included in WACCM simulations.

H_2 and H_2O emission profiles (kg/km/flight) are interpolated with 1-km vertical resolution (Figure 1a). The spike in emissions at 28 km is due to the spacecraft transition into rocket mode. The total amount of H_2O produced from a single flight is estimated to be 6×10^5 kg (assuming completely oxidized H_2) with about 4×10^5 kg emitted into the stratosphere (above 17 km). The projected 10^5 flights per year would deposit 4×10^{10} kg of H_2O in the stratosphere every year. To get a sense of how large a perturbation this represents, the yearly emissions are compared to the total amount of stratospheric water. Assuming a uniform mixing ratio of 4.5 parts per million by volume (ppmv) of H_2O above 100 hPa (17 km), there is 1.5×10^{12} kg of H_2O in the stratosphere. The projected 10^5 flights would emit approximately 3% of the current stratospheric H_2O burden every year. Assuming a constant flight frequency and a 3-year lifetime of the H_2O, when emitted above 100 hPa, this would increase globally averaged stratospheric H_2O by approximately 9%. The actual steady-state perturbation of H_2O due to these emissions in WACCM above 100 hPa is 10%; however, the local perturbation would be much larger and increase with height.

Estimating a NO_X emission profile for the Skylon vehicle is problematic. Several flight phases must be considered: H_2 burned with air as a jet fuel, H_2 burned with liquid oxygen as a rocket fuel, and heating of air due to aerodynamic interactions. It is important to note that we consider the shock heating of air during reentry as an emission. When air is heated to temperatures exceeding 1800 K, as in a jet engine or behind the shock wave around a spacecraft during reentry, NO_X is produced through the extended Zeldovich mechanism [*Zeldovich et al*., 1947]. This mechanism is exponentially dependent on temperature so that representative temperatures are required in order to calculate the thermally produced NO_X. Detailed estimates of the NO_X emissions have not yet been calculated by the rocket designers [*R. Varvill*, 2015, personal communication]. For this study, reliable estimates of NO_X emissions from jet and rocket engines are scaled to the Skylon vehicle with the caveat that our estimates have high uncertainty. *Lee et al*. [2010], using the International Civil Aviation Organization (ICAO) emissions databank, estimated that 14 ± 3 g of NO_X are produced for every kilogram of fuel combusted in jet engines. Emissions may be lower at supersonic speeds and are also a function of the temperature difference between high pressure (~100 atmospheres) liquid H_2 and jet fuel. Most of the engines in the ICAO databank use jet fuel with a 2:1 H:C ratio. The higher fuel density must be taken into consideration in the NO_X estimates from H_2 combustion. For complete combustion in the jet engine air-burning phase, two hydrogen and one carbon atoms (14 g/mol) react with three oxygen atoms. For a

pure H_2 fuel at complete combustion, three oxygen atoms will oxidize six hydrogen atoms (6 g/mol). Thus, from a stoichiometric perspective, burning 1 kg of jet fuel requires as much air as 6/14 kg of H_2 fuel. Thus 6/14 kg of H_2 fuel is assumed here to produce 14 g (11–17) of NO_X during the air-burning phase. Alternatively, using the heat of combustion per fuel mass to scale the NO_X production gives consistent results that are within the uncertainty range. The total production of NO_X during the air-burning Skylon ascent is estimated to be 1400 ± 300 kg, although we acknowledge this range does not encompass all the uncertainties in the assumptions.

Zero NO_X emission is assumed during the liquid oxygen burning phase of ascent. NO_X would only be produced in H_2-fueled rocket engines in significant amounts (>0.01% of total flow) in afterburning reactions, which occur when ambient air is entrained into the hot underoxidized plume [*Brady et al*., 1997]. Afterburning is generally not a significant factor for rocket engines above the tropopause. Therefore it is assumed that during this phase of flight, at altitudes greater than 28 km, significant NO_X production is unlikely.

Finally, NO_X is also produced in the shock wave during spacecraft reentry. Using analytic approximations and a numerical integration, *Park* [1976] calculated that the NO_X produced during a Space Shuttle reentry is 4.5–9% of the mass of the spacecraft. *Park and Rakich* [1980] later updated this value to 17.5 ± 5.3% of the spacecraft mass, with a peak emission at 68 km. While the predicted Skylon mass is comparable to the Space Shuttle mass, the Skylon reentry flight path is different from that of the Shuttle, and this would affect NO_X production. Skylon is expected to require more time above 5 km/s during reentry than the Shuttle did, which would tend to produce more NO_X. However, these high speeds would occur at a higher altitude than for the Space Shuttle, which would tend to decrease NO_X production [*Park*, 1976]. Given the compensating factors, and in the absence of actual flight data, Skylon is assumed to have the same vertical profile of reentry NO_X emission as the Space Shuttle, with the total values scaled by vehicle mass. The estimated total amount of NO_X produced during reentry is therefore 9880 ± 2760 kg per flight. This range does not encompass the uncertainty in all the assumptions made, and thus the stated value of NO_X production is considered only representative. The estimated altitude profiles of NO_X emissions from the ascent and reentry phases are shown in Figure 1b.

Park [1976] compared NO_X formation between the Space Shuttle and meteorites based on the total mass entering the top of the atmosphere. Assuming the natural formation rate of upper atmospheric NO_X is from 5.7×10^7 kg of meteorites producing their weight in NO_X every year [*Park*, 1976], then 10^5 Skylon flight reentries would produce a factor of 20 more NO_X than natural production from meteorites. Meteorites produce roughly 5× more NO_X per mass than the Space Shuttle due to their much higher velocity when entering the atmosphere.

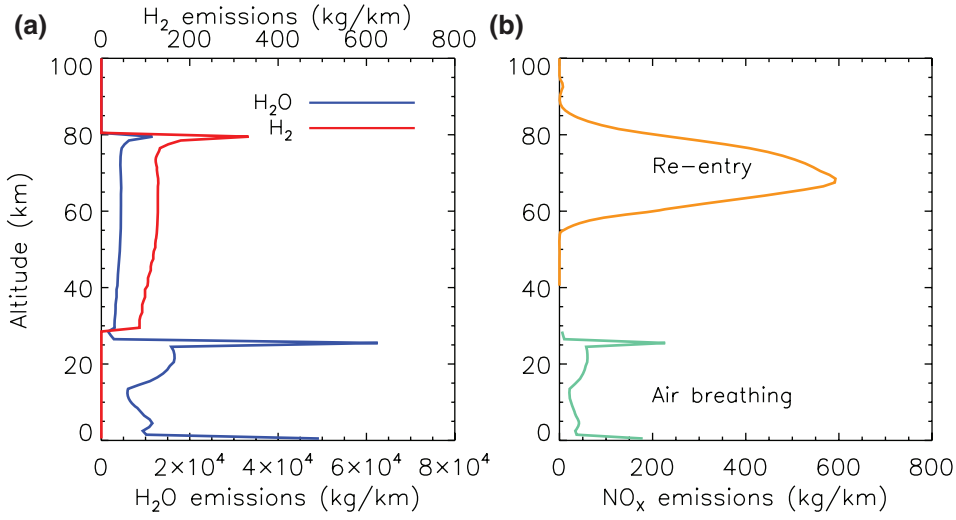

Figure 1. (a) Vertical profiles of H_2O and H_2 emitted from the air-breathing and rocket ascent of one Skylon rocket launch. (b) Vertical profiles of NO_X emissions from the air-breathing ascent and reentry of one Skylon rocket.

Table 1. Simulation Descriptions and Globally Averaged Total-Column O_3 Depletion and Effective Radiative Forcing (ERF) Compared to a Zero-Emission Reference Case From the NOCAR and WACCM Models

Simulation	Flights (per year)	Air-Breathing 0–28 km	Rocket 28–80 km	Reentry 50–100 km	ΔO_3 (DU) NOCAR	ΔO_3 (DU) WACCM	ERF(W/m^2)
1	10^5	NOx		NOx	−1.1	−1.4*	−0.01
2	10^5			NOx	−0.7	−0.1	0.00
3	10^5	NOx			−0.5	−0.5	0.01
4	10^5	H_2O	H_2O		−0.5	0.4	0.08
5	10^5	H_2O	H_2, H_2O[b]		−0.4	−0.9	0.04
6	10^5	NOx H_2O	H_2O	NOx	−1.5	−1.3*	0.06
7	10^5	NOx H_2O	H_2, H_2O[b]	NOx	−1.5	−1.4*	−0.01
8	$3x10^5$	NOx H_2O	H_2, H_2O[b]	NOx	−3.9	−3.5*	0.09*
9	10^6	NOx H_2O	H_2, H_2O[b]	NOx	Not Run	−11.0*	0.28*
10	10^4	NOx H_2O	H_2, H_2O[b]	NOx	−0.2	Not Run	0.01

Columns 3–5 indicate the species emitted according to the vertical profile in Figure 1 during that mode of flight. Blanks indicate no emissions during this mode. Numbers with an asterisk are significant at the 95% levels using Monte Carlo resampling. Uncertainty estimates from the NOCAR model are not representative of the actual uncertainty in the estimates and not included.
[b] Assumes a 25:75 mole fraction of H_2:H_2O emitted in plume.

3. Model Descriptions

Table 1 summarizes the simulations that are run and includes the rocket emissions considered in each case. The Community Earth System Model (CESM v1.0.6) using the WACCM model [*Marsh et al*., 2013] is used to simulate these emissions. WACCM was chosen because the model domain extends higher than most climate models (140 km) and it can include interactive chemistry. Simulations are run with fixed sea surface temperatures and perpetual year 2000 anthropogenic emissions and CO_2 concentrations at $1.9 \times 2.5°$ resolution with 66 vertical levels using a hybrid sigma coordinate system. Cases with different emissions and flight frequency are compared to a zero-emission control case. Vertical emission profiles of H_2O, H_2, and NO_X are included into two model horizontal grid cells spanning the equator. An equatorial launch is assumed because the energy required to put a rocket into orbit increases with launch latitude. Sensitivity tests are also run with the NOCAR model as these tests would be computationally expensive using WACCM. The NOCAR model is used to evaluate the sensitivity of our results to launch location, chlorine and greenhouse gas concentrations, emissions products, and number of launches per year.

Including emissions into global model grid cells effectively dilutes the concentration of emissions compared to an actual rocket plume. The size of the equatorial grid cells is roughly 200×250 km^2, which is about 1000 times larger in area than a rocket plume. The concentrations used in the model are thus 1000 times less than exist in the initial rocket plumes. Another assumption is that the emissions fill the grid cell before any chemical changes take place. Studies such as *Lohn et al*. [1999] and *Ross et al*. [1997] have looked into O_3 depletion and other atmospheric effects inside rocket plumes. *Lohn et al*. [1999] found that solid rocket motor exhaust plumes from Titan class rockets destroy all of the O_3 in the wake of the rocket. These predictions were verified by in situ plume measurements [*Ross et al*., 1997]. The ozone-depleted regions are several square kilometers in size and last about an hour before dissipating to background concentrations. It is expected that plume chemistry will affect the composition and abundance of the rocket emissions that exist at the grid scale after the plume disperses. However, for the Skylon emissions, the amount of excess H_2 emitted during rocket mode that is oxidized in the plume versus the amount present at the grid scale is unknown. Thus, the limiting cases are explored, one in which all the excess H_2 is immediately oxidized (simulation 4) and one in which it all persists to the grid scale (simulation 5).

The sensitivity of two of our assumptions are tested with the NOCAR model; specifically that H_2O and H_2 are the only relevant HO_Y species emitted, and secondly, that year 2000 greenhouse gas and chlorine levels are appropriate choices for this study. Some hydrogen will be emitted as HO_Y species, although it is likely to be very small. *Swain et al*. [1990] measured H_2O_2 in hydrogen burning engine exhaust and found it to be

Table 2. Sensitivity Studies with the NOCAR Model Simulating the Inclusion of HO_X and H_2O_2 in Simulation 7

Species	Mole Fraction (%)	O_3 Anomaly (DU) Compared to Simulation 7
HOx	1	−0.01
HOx	0.1	−0.02
H_2O_2	1	−0.05
H_2O_2	0.1	−0.01

undetectable under normal operating conditions and up to 1000 ppmv under extremely inefficient conditions when the fuel to air ratio was around 5. Despite this, we simulate some of the hydrogen emitted as HO_X or H_2O_2 using the NOCAR model. Note that due to the family chemistry scheme in NOCAR, we cannot emit OH directly, but instead emitted an equivalent quantity as HO_X, which should produce the same amount of ozone destruction. The H_2O_2 can be emitted directly because it is long lived. Table 2 displays the global mean total column ozone changes relative to simulation 7 (Table 1) with and without these emissions. Including these emissions, even at relatively high amounts (1% mole fraction), results in essentially no change in O_3 loss. The global mean total column ozone loss in these simulations is within 0.05 Dobson Units (DU) of the base case (simulation 7). Thus, these species (OH and H_2O_2) are not important to include in the WACCM simulations.

The WACCM simulations assume year 2000 conditions; however, we note that flights of the Skylon space plane, especially at rates assumed in this paper, are decades away at best. Future levels of greenhouse gases and chlorine are estimated to be much higher and lower, respectively, than in the year 2000 [*IPCC*, 2013]. Thus, we also test the sensitivity of ozone loss on greenhouse gas and chlorine levels with the NOCAR model. These results are shown in Table 3. Using year 2100 chlorine levels increases the global total column ozone loss by 6% compared to simulation 7. Under a lower chlorine concentration, NO_X increases destroy more ozone due to reduced formation of chlorine nitrate. However, water vapor increases induce less ozone destruction from polar stratospheric cloud (PSC) increases due to decreased chlorine. The net effect is increased ozone losses from rocket emissions. Increasing greenhouse gas levels to year 2100 offsets some of this extra loss and the sign of the final change depends on the relative amounts of the three greenhouse gases in the scenario. CO_2 increases cause the rocket-induced change to increase, while CH_4 and N_2O increases cause it to decrease. However, the changes are relatively small in all cases using the NOCAR model and we consider our WACCM simulations using year 2000 values as representative of any time between now and year 2100.

4. Stratospheric Ozone and Temperature Perturbations

Our base case scenario for 10^5 flights per year is simulation 7 in Table 1, which includes NO_X, H_2, and H_2O emissions. The components of the emissions are modeled separately in simulations 1–6 to better understand the changes to O_3. Plots of the O_3 change due to the individual emission components can be found in the supplement. Preliminary WACCM simulations using a different emissions profile than Figure 1 and 10^4 flights per year did not produce any statistically significant global changes to the atmosphere. At 10^5 flights per year, as seen in simulation 7, stratospheric NO_X concentrations increase by 0.3–3 parts per billion (ppb)

Table 3. Simulations with the NOCAR Model Testing the Sensitivity of the Results on Greenhouse Gas (GHG) and Chlorine (Cl_Y) Levels

GHG Year Level	Cl_Y Year Level	O_3 Anomaly (DU)	Change(%)
2000	2000	−1.48	—
2000	2100	−1.57	6
2100 (RCP45)	2100	−1.53	3
2100 (RCP85)	2100	−1.41	−5

The top row is equivalent to simulation 7 in Table 1. Chlorine and GHG levels at 2100 assuming scenario RCP45 and RCP85 [*van Vuuren et al*., 2011].

and stratospheric H_2O increases by 0–3 ppm. At this and higher flight frequencies significant changes occur in the stratosphere as shown in Figure 2.

At 10^5 flights per year O_3 decreases significantly at all latitudes at altitudes above about 25 km and above 20 km at the poles as seen in simulation 7 (Figure 2a). The overlaid hatching (Figure 2a) indicates statistical significance from two different tests. As seen in Table 1, this depletion in O_3 is predominantly due to catalytic destruction by NO_X [*Crutzen*, 1970]. Our simulations with just NO_X emissions (simulation 1) had almost the same amount of ozone destruction as the simulation with NO_X, H_2O, and H_2 (simulation 7), and much more than simulations without NO_X (simulations 4 and 5). Both sources of NO_X, air-breathing ascent and reentry, contribute to the destruction of O_3 as seen in simulations 2 and 3. However, the models disagree about the relative contribution from these two emission sources. The NOCAR model attributes more O_3 loss than WACCM does to NO_X created in the mesosphere during reentry (simulation 2). In addition, including H_2 emissions may further reduce total O_3 compared to H_2O emissions alone in WACCM simulations. Note that including H_2 emissions does not exacerbate O_3 loss in the NOCAR runs; in fact O_3 loss is lessened between simulations 4 and 5. Moreover, assuming H_2O emissions alone seems to lead to an increase in O_3 in WACCM; however these results are within the range of internal variability.

Below this region of destruction by NO_X is a global layer of O_3 enhancement between 18 and 24 km (Figure 2a), which can be explained through smog chemistry. The air-breathing ascent emits NO_X throughout the troposphere and in the lower stratosphere at the equator. NO_X emissions in the troposphere produce O_3 through smog chemistry [*Liu et al*., 1980], which can also occur in the lowermost stratosphere. In addition ozone increases can occur from the "self-healing" effect (i.e., increased O_3 production from increased UV penetration due to O_3 losses above). O_3 increases in the tropical tropopause region are not seen in the simulation with only reentry NO_X (see Figure S2, Supporting Information).

There are other competing processes due to the H_2O emissions that affect O_3 as well. The emitted H_2O radiatively cools the stratosphere by a degree or less below 45 km and 1–3° above (Figure 2c and 2d). Although Figure 2 includes NO_X and H_2 emissions, similar cooling is present in simulations only considering H_2O emissions (see Figure S4). Lower temperatures cause chemical reaction rates between O and O_3 to become slower, thereby suppressing O_3 loss and causing a positive anomaly below 40 km. Above about 40 km, this effect is more than offset by increased depletion of O_3 due to an enhanced HO_X catalytic cycle [*Crutzen*, 1969; *Lary*, 1997]. This is roughly consistent with modeling efforts of *Evans et al*. [1998], who found that increased CO_2 and H_2O in the upper atmosphere lead to net O_3 loss above 50 km and production below. They also see some net loss around the tropopause, again roughly consistent with WACCM and the NOCAR model simulation 4, which only assumes H_2O emissions (see Figure S4). Similarly, *Tian et al*. [2009] found that an increase of 2 ppm of H_2O in the stratosphere affected O_3 both chemically and radiatively. They found that an increased HO_X cycle destroys stratospheric O_3, while the radiative cooling from increased H_2O increases stratospheric O_3. However, when cooling exceeds 5 K in their model, the total column O_3 at high latitudes decreases rather than increases. Furthermore, *Stenke and Grewe* [2005] also found that increased stratospheric H_2O in their model increased HO_X chemistry and destroyed O_3; however the enhancement in OH decreased the efficiency of O_3 destruction by the NO_X cycle.

The global total column O_3 abundance in simulation 7 decreases by 1.4–1.5 DU (Table 1), with the highest O_3 destruction occurring in the Antarctic (Figure 3a), although destruction in the tropics contributes more to the globally averaged total column O_3 loss due to the larger area of the tropics. The polar regions are highly variable in WACCM as indicated by the gray shading. The red line in Figure 3 indicates results from the NOCAR model. The NOCAR model has more O_3 loss than WACCM at the poles; however, the latitudinal dependencies are similar. NOCAR has annually repeating planetary and gravity wave fluxes in the troposphere, which limits the interannual variability, and thus we do not add uncertainty ranges due to variability.

Simulation 8 (Figure 3b) has 3× higher flight frequency than simulation 7 and roughly 3× more O_3 loss at most latitudes. However, in the Arctic, simulation 7 (Figure 3a) shows no ozone loss on average, while simulation 8 (Figure 3b) shows 7 DU of ozone loss. This difference is likely a consequence of cooler stratospheric temperatures having a nonlinear effect on O_3 destruction [*Tian et al*., 2009]. *Tian et al*. [2009] found that chemical and radiative effects of a 2 ppmv increase of H_2O lead to net increases in total column O_3 in the Arctic. However, when the radiative cooling exceeded 4 K, they found that the total column O_3 decreased.

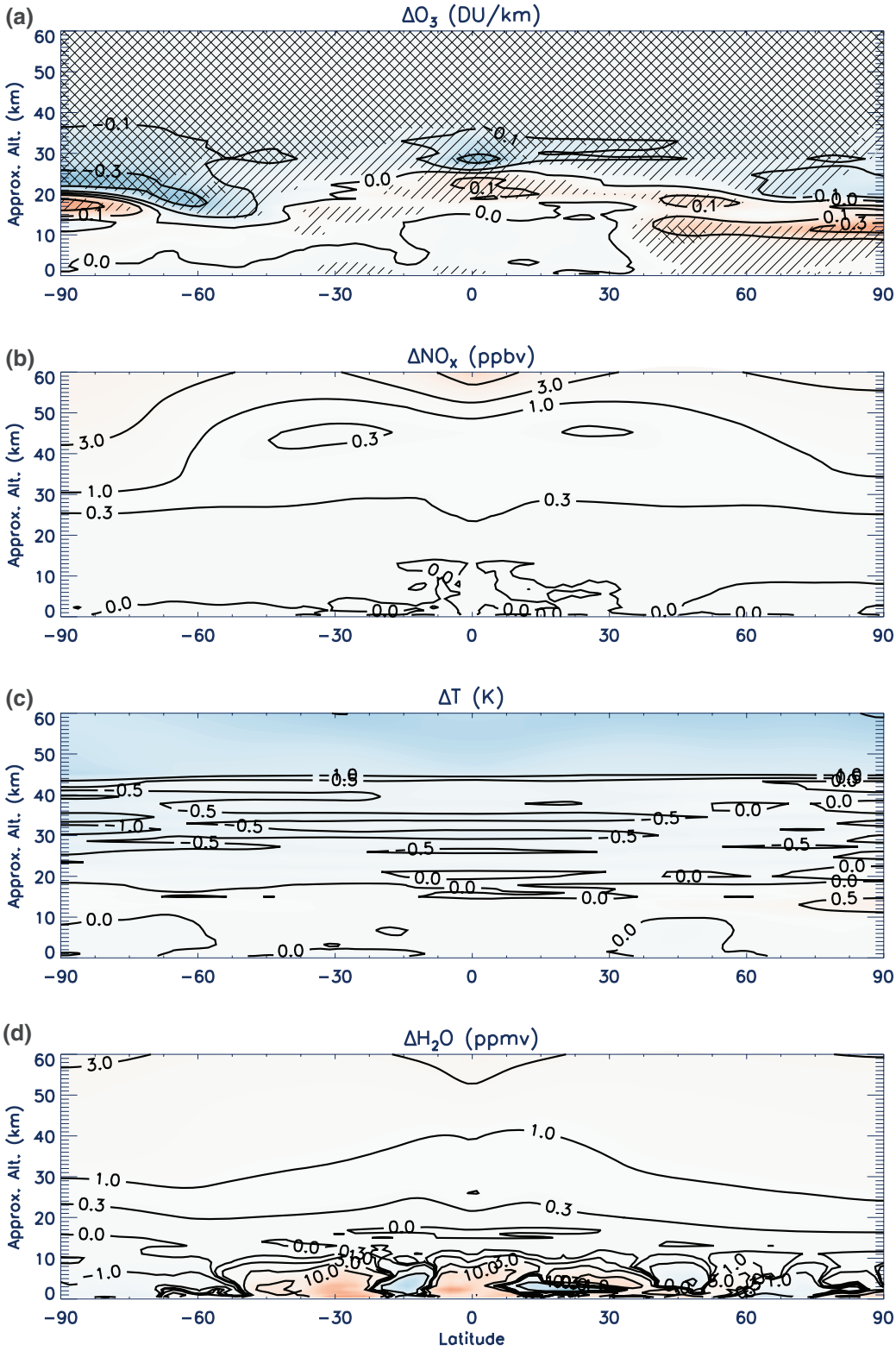

Figure 2. Changes to O_3 (a), NO_X (b), T (c), and H_2O (d) due to 10^5 Skylon rocket flights per year from the WACCM simulation 7 shown in Table 1. Vertical emissions of H_2O, H_2, and NO_X are added into two model horizontal grid cells spanning 2°S to 2°N. The results are anomalies referenced to the control simulation for years 6–60 of a 60-year simulation. Lines at an angle of 45° (from horizontal) are significant at the 95% level using a Student's *t*-test. Lines at an angle of −45° (from horizontal) are significant at the 95% level using Monte Carlo resampling with 1000 samples.

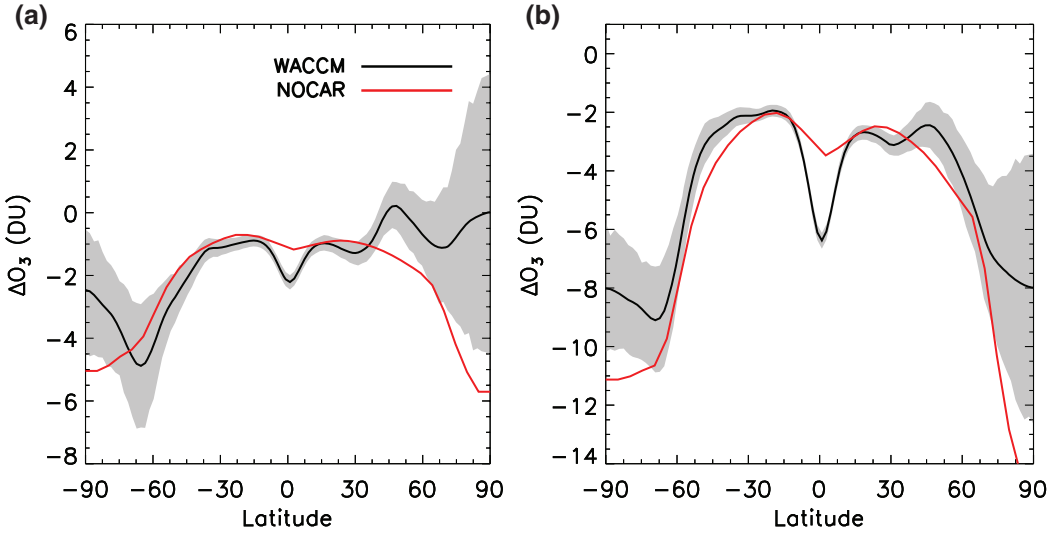

Figure 3. Latitudinal profiles of total column O_3 anomalies from simulations 7 (a) and 8 (b) shown in Table 1. Simulation 8 (b) is identical to simulation 7 (a) except with 3× larger flight frequency. Years 6–60 of a 60-year WACCM simulation are averaged to calculate the WACCM results (black lines). Gray shaded region indicates the 95% confidence interval estimated using Monte Carlo sampling. The red lines are results from the NOCAR model.

This is consistent with our findings from WACCM. Simulation 7 (Figure 3a) has no net O_3 loss in the Arctic, however, simulation 8 (Figure 3b), which has a higher flight frequency and cooler stratospheric temperatures (see Figure S7), has significant net loss.

The seasonal cycle of O_3 destruction in WACCM (Figure 4a) due to constant rocket emissions throughout the year is shown along with the globally averaged O_3 anomaly (Figure 4b). The largest O_3 depletion occurs in austral spring in the Antarctic. WACCM (Figure 4a) has slight positive O_3 anomalies for much of the year in the northern mid latitudes, in the Arctic, and in the Antarctic summer that are not seen in the NOCAR model (see Figure S8). However, the NOCAR global mean total column O_3 anomaly is within the uncertainty of the WACCM simulation in all seasons (Figure 4b). Ozone loss in the polar regions has large variability in WACCM simulations (Figure 4c) which leads to the large uncertainty ranges near the poles, as seen in Figure 3.

The relationship between O_3 column depletion and rocket launch frequency is quasilinear. Emissions from 10^5 flights per year decrease O_3 by 1.4–1.5 DU, 3×10^5 flights per year decrease O_3 by 3.5–3.9 DU, and 1×10^6 flights per year decrease O_3 by 11 DU. Results from the NOCAR model agree well with the WACCM results. The NOCAR model also indicates that moving the launch location to any latitude outside the tropics produces similar globally averaged column O_3 anomalies, although the maximum anomaly tends to be at the pole in the hemisphere of emissions (not shown). Emissions near the equator have similar maxima at the two poles in the NOCAR model.

Additional impacts of 10^5 rocket launches per year include enhanced polar mesospheric clouds (PMCs) over both poles and enhanced Antarctic PSCs as seen in Figure 5. PMC fractions increase by about 20% and are similar in each hemisphere. Antarctic PSC fractions also increase by about 20%. We note, however, that the multiyear average control simulation does not show Arctic PSCs, and we do not simulate Arctic PSC increases. This is likely a consequence of large variability in the Arctic; only during very cold years will PSCs be present, and this is not well represented in our simulations, which consider 54 years in the averages. Other studies [*Feck et al*., 2008; *Vogel et al*., 2011] demonstrate that with increased H_2O there is increased PSC formation and associated ozone destruction in the Arctic spring, especially during cold winters. *Vogel et al*. [2011] show that the springtime Arctic ozone depletion depends on the background chlorine concentration. Their ozone loss anomaly due to enhanced water vapor and decreased stratospheric temperatures is reduced from 6 to 3.4 DU under conditions from current chlorine to 40% less chlorine loading. However, we note that it is difficult to compare the results from *Vogel et al*. [2011] with our study as the majority of ozone destruction in our simulations occurs at tropical and mid latitudes and the mechanisms are different. In addition, our simulations include catalytic destruction due to NO_X emissions as well as water vapor.

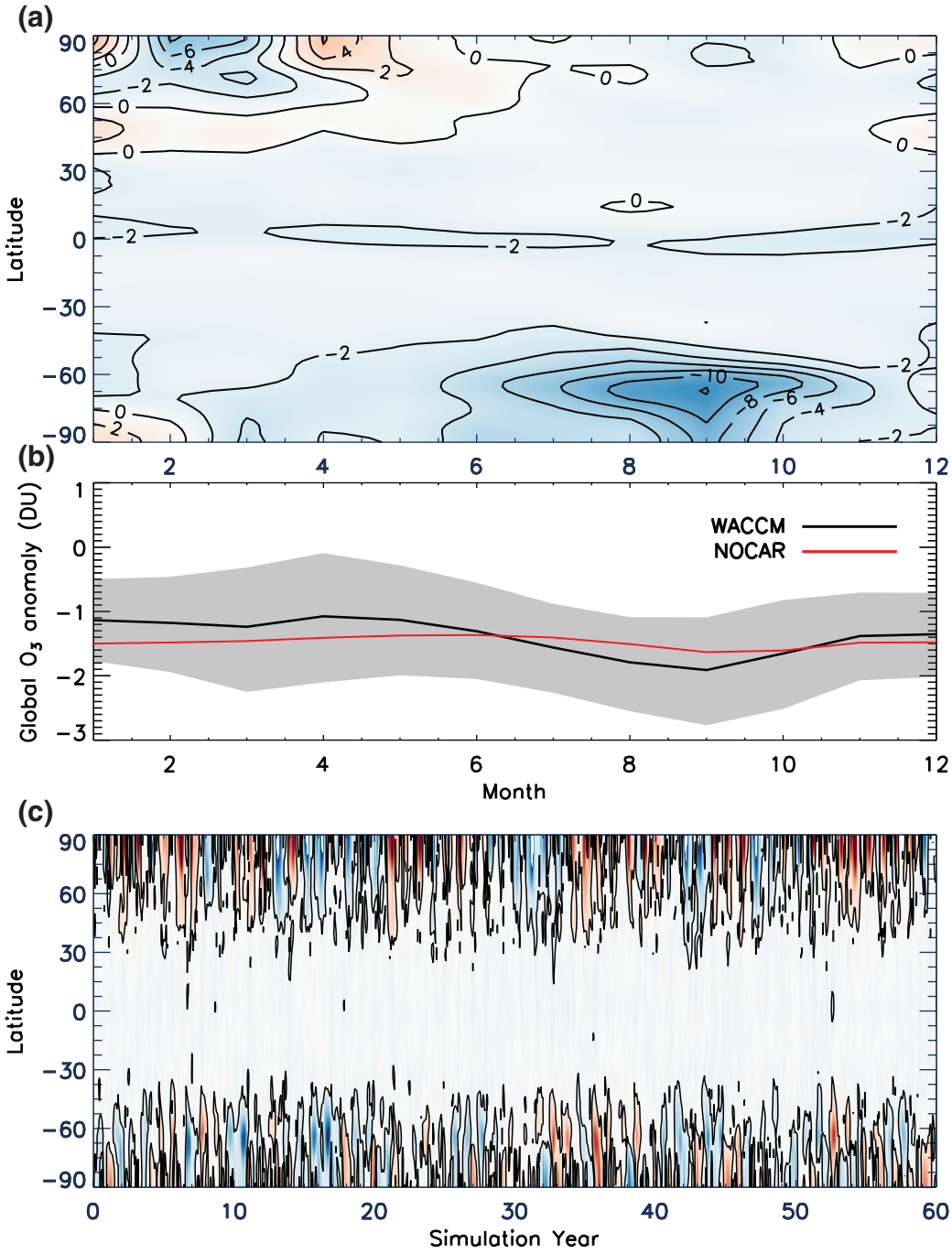

Figure 4. (a) Seasonal cycle of total column O_3 depletion (DU) by latitude from WACCM. (b) Globally averaged seasonal cycle of total column O_3 depletion from WACCM and NOCAR models. The gray shading is the 95% confidence interval as estimated by Monte Carlo sampling. The anomalies shown in panels a and b are averaged over years 6–60 of a 60-year simulation. C) Time series of total column O_3 depletion by latitude in WACCM. The contour lines indicate ±10 DU. All panels are from simulation 7 shown in Table 1.

The PMC enhancement in our simulations is relevant to the discussion about increasing trends in PMCs since the 1970s. These trends are associated with increasing water vapor and decreasing temperatures [*Hervig et al*., 2016] and have been ascribed to increasing greenhouse gases [*Thomas and Olivero*, 2001]. *Siskind et al*. [2013] suggested a link between space traffic and increased PMC formation in 2011 and 2012. Our simulations suggest a large number of rocket launches could greatly increase PMC formation in the future. The PMC enhancements in our simulations are dependent on launch latitude and preferentially occur in

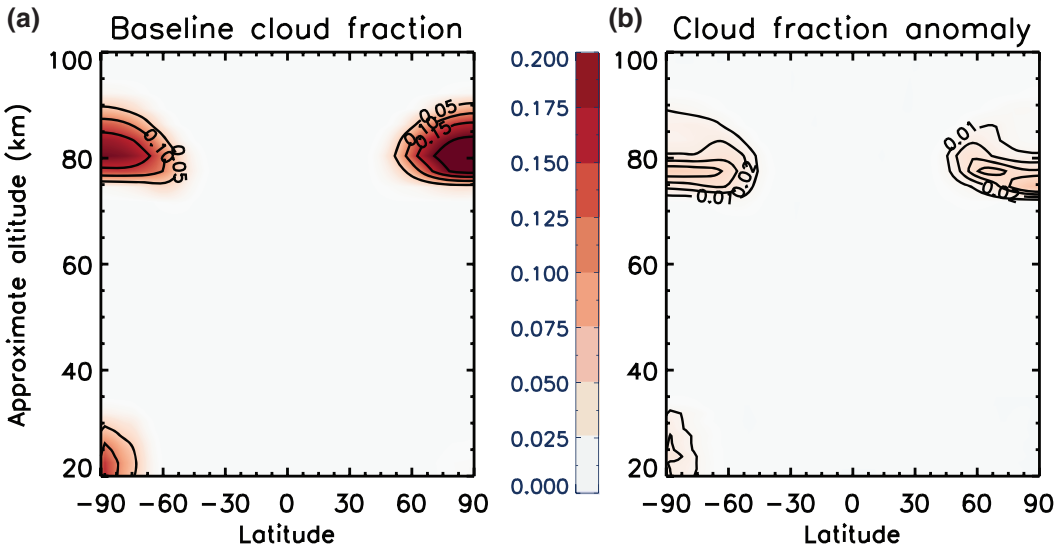

Figure 5. (a) Zonally averaged, annual-mean cloud fractions from the control simulations showing PMCs near 80 km and PSCs near 20 km. (b) Cloud fraction anomalies from simulation 7 shown in Table 1. PMC and PSC fractions increase by approximately 20% in the Antarctic due to the rocket emissions.

the hemisphere of launch during the summer season. Emissions in the winter season do not significantly enhance PMC formation. In the mesosphere this dependence is due to the mean mesospheric winds carrying the H_2O perturbation toward the winter hemisphere and away from where PMCs form in the summer hemisphere, whereas high-latitude launches during summer deposit H_2O directly where PMCs form. The PSC increase contributes to the modeled O_3 destruction between 20 and 30 km over Antarctica. However, the PSC contribution to total global O_3 depletion is small compared to the depletion caused by gas-phase catalytic chemistry. Furthermore, the contribution of O_3 loss from PSCs depends on the background chlorine and bromine levels. This simulation uses year 2000 chlorine and bromine concentrations, and likely is an overestimate of the PSC-induced heterogeneous O_3 destruction in future decades when stratospheric chlorine and bromine levels are expected to be lower. However, NOCAR results discussed in Section 3 indicate that different chlorine and greenhouse gas concentrations have a small effect, roughly a few percent, on the global mean total column ozone destruction from these emissions.

Since these simulations have fixed sea surface temperatures, the effective radiative forcing (ERF) is calculated directly as the difference in the top of the atmosphere net radiation between the control and experimental simulations. The ERF from 10^5 Skylon rocket launches per year is not significant; however, 3×10^5 and 10^6 launches per year cause statistically significant radiative forcing of 0.09 and 0.28 W/m^2, respectively (Table 1). Scaling these results down to 10^5 launches per year gives an ERF of about 0.03 W/m^2. This is roughly three times larger than the forcing value obtained from the simulation with 10^5 flights, but within the range of variability in that simulation. The radiative forcing is largely caused by the increase in stratospheric water vapor.

5. Conclusions

WACCM model simulations of estimated Skylon rocket emissions indicate that 10^5 or more flights per year, as proposed to build a space-based power system, significantly affect the atmosphere in several ways. Global stratospheric O_3 decreases by approximately −1.4 DU in comparison to the reference simulation. This depletion is about 10% of the historic peak depletion of global total column ozone in the 1990s due to anthropogenic emissions of synthetic gases [*Pawson et al.*, 2014]. The O_3 depletion is mostly (~75%) due to NO_X emissions. At 10^6 flights per year, the effects on O_3 are more robust, with estimated O_3 loss enhanced by about an order of magnitude relative to 10^5 flights per year.

Other climate effects include tropospheric O_3 increases, PSC and PMC increases, and slightly positive ERF. The radiative forcing is mostly caused by the increased stratospheric and mesospheric water vapor. The

enhancement in PSC fraction contributes to O_3 loss, although the contribution to global loss is smaller than that of destruction from gas-phase catalytic chemistry. The O_3 perturbation is the largest and likely the most significant impact from these flights. In comparison, the other calculated impacts are small compared to natural variability or the consequences of other anthropogenic activities, or are statistically insignificant at least when considering up to 10^5 flights per year.

It is useful to compare the calculated Skylon ERF with estimates of the ERF associated with black carbon emitted by hydrocarbon-fueled rocket engines. *Ross et al*. [2010] estimated that a scenario of 10^3 flights per year of a small suborbital hydrocarbon burning rocket would produce ERF of 0.04 W/m^2, approximately the same as the Skylon scenario of 10^5 orbital flights per year. The hydrocarbon fuel mass used in the suborbital rocket scenario is only approximately 0.03% of the H_2 fuel mass used in 10^5 Skylon orbital flights, yet the predicted ERF is similar. This comparison demonstrates the large differences in space transport impacts associated with different fuels and points out the importance of evaluating all rocket engine types for the purposes of future policy and rocket design.

Effects from these rocket flights are expected to be transient, persisting only a few years after the high flight rates cease. The stratospheric circulation will ultimately remove the excess H_2O and NO_X. The scenario modeled here is just one example of a dramatic increase in rocket flight frequency. Although a specific launch vehicle propellant and entry emissions are assumed, the results are representative of any H_2-fueled launch vehicle with similar mass.

Our results show that H_2-fueled launch vehicles can have significant global impacts at sufficiently high emission or launch rates. Compared with estimates of the global impacts of a hydrocarbon-fueled rocket [*Ross et al*., 2010], our results substantiate assertions that, by some measures, H_2-fueled rockets are indeed "clean," though such conclusions must be made with caution. Obtaining our results required the use of a modern atmospheric chemistry/climate model because the emissions are distributed over large ranges in space and time and interact with complex chemical and dynamical features of the climate system. We conclude that it is important to make a more detailed examination of the potential global impacts of all rocket propellant types whose use might be expected to grow significantly in the future, including kerosene-fueled and solid rocket motors, both of which can be expected to have a much greater global impact per launch than H_2-fueled systems of the kind modeled here.

Acknowledgments
The authors would like to thank Keith Henson of the L5 Society for suggesting this study. They also thank Keith Henson and Richard Varvill of Reaction Engines Ltd for their helpful discussions in the development of this paper. This study was supported in part by NOAA's Climate Program Office. This paper does not analyze any observational data; however, simulation output can be requested from the corresponding author.

References

Brady, B. B., L. R. Martin, and V. I. Lang (1997), Effects of launch vehicle emissions in the stratosphere, *J. Spacecr. Rockets*, *34*, 774–779, doi:10.2514/2.3285.

Colasurdo, G., D. Pastrone, and L. Casalino (1998), Optimal performance of a dual-fuel single-stage rocket, *J. Spacecr. Rockets*, *35*, 667–671, doi:10.2514/2.3383.

Crutzen, P. J. (1970), The influence of nitrogen oxides on the atmospheric ozone content, *Q. J. R. Meteorol. Soc.*, *96*, 320.

Crutzen, P. J. (1969), Determination of parameters appearing in the "dry" and the "wet" photochemical theories for ozone in the stratosphere, *Tellus*, *XXI*, 368–388.

Evans, S. J., R. Toumi, J. E. Harries, M. P. Chipperfield, and J. M. Russell (1998), Trends in stratospheric humidity and the sensitivity of ozone to these trends, *J. Geophys. Res.*, *103*, 8715–8725.

Feck, T., J.-U. GrooB, and M. Reise (2008), Sensitivity of Arctic ozone loss to stratospheric H2O, *Geophys. Res. Lett.*, *35*, L01803, doi:10.1029/2007/GL031334.

Henson, K. (2014), Solving economics, energy, carbon, and climate in a single project. *2014 IEEE Conf*. *Technol*. *Sustainab*. (*SusTech*), 24–26 Jul., 203–208.

Hervig, M. E., U. Berger, and D. E. Siskind (2016), Decadal variability in PMCs and implications for changing temperature and water vapor in the upper mesosphere, *J. Geophys. Res. Atmos.*, *121*, 2383–2392, doi:10.1002/2015JD024439.

IPCC (2013), *Climate Change 2013: The Physical Science Basis*, Cambridge Univ. Press, Cambridge, U. K., 1535 pp.

Johnston, H. (1971), Reduction of stratospheric ozone by nitrogen oxide catalysts from supersonic transport exhaust, *Science*, *173*, 517–522.

Khan, M. F., Z. A. Quadri, P. S. Kulkarni, U. Guven, S. P. Bhat, and K. Sundarraj. (2013), CFD simulation of a liquid rocket propellant (LH2\LOx) combustion chamber. *15th Annual CFD Sympos*., Indian Inst. Sci., Bangalore, India, 9–10 Aug.

Lary, D. J. (1997), Catalytic destruction of stratospheric ozone, *J. Geophys. Res.*, *102*, 21,515–21,526.

Lee, D. S., et al. (2010), Transport impacts on atmosphere and climate: Aviation, *Atmos. Environ.*, *44*, 4678–4734.

Li, J., Z. Zhao, A. Kazakov, and F. L. Dryer (2004), An updated comprehensive kinetic model of hydrogen combustion, *Int. J. Chem. Kinet.*, *36*, 566–575, doi:10.1002/kin.20026.

Liu, S. C., D. Kley, M. McFarland, J. D. Mahlman, and H. Levy (1980), On the origin of tropospheric ozone, *J. Geophys. Res.*, *85*, 7546–7552.

Lohn, P. D., E. P. Wong, T. W. Smith Jr., J. R. Edwards, and D. Pilson. (1999), Rocket exhaust impact on stratospheric ozone, *Tech. Rep. Submitted to U.S. Air Force Space and Missile Systems Center Environmental Management Branch SMC/AXFV*. [Available at http://oai.dtic.mil/oai/oai?verb=getRecord&metadataPrefix=html&identifier=ADA414282]

Marsh, D. R., M. J. Mills, D. E. Kinnison, J.-F. Lamarque, N. Calvo, and L. M. Polvani (2013), Climate change from 1850 to 2005 simulated in CESM1(WACCM), *J. Clim.*, *26*(19), 7372–7391, doi:10.1175/JCLI-D-12-00558.1.

Martin, T., R. Varvill, and A. Bond. (2008), Solar power satellites and space planes. *Tech. Rep.*, Reaction Engines Ltd, Oxfordshire, U.K. [Available at http://www.reactionengines.co.uk/tech_docs.html]

Park, C. (1976), Estimates of nitric oxide production for lifting spacecraft reentry, *Atmos. Environ.*, *10*, 309–313.

Park, C., and J. V. Rakich (1980), Equivalent-cone calculation of nitric oxide production rate during space shuttle re-entry, *Atmos. Environ.*, *14*, 971–972.

Pawson, S., W. Steinbrecht, A. J. Charlton-Perez, M. Fujiwara, A. Y. Karpechko, I. Petropavlovskikh, J. Urban, and M. Weber. (2014), Chapter 2: Update on global ozone: Past, present, and future. *Scientific Assessment of Ozone Depletion: 2014, Global Ozone Research and Monitoring Project, Rep. No. 55*, World Meteorol. Org., Geneva, Switzerland.

Portmann, R. W., and S. Solomon (2007), Indirect radiative forcing of the ozone layer during the 21st century, *Geophys. Res. Lett.*, *34*, L02813.

Ross, M., D. Toohey, M. Peinemann, and P. Ross (2009), Limits on the space launch market related to stratospheric ozone depletion, *Astropolitics*, *7*(1), 50–82.

Ross, M., M. Mills, and D. Toohey (2010), Potential climate impact of black carbon emitted by rockets, *Geophys. Res. Lett.*, *37*, L24810, doi:10.1029/2010GL044548.

Ross, M. N., J. R. Benbrook, W. R. Sheldon, P. F. Zittel, and D. L. McKenzie (1997), Observation of stratospheric ozone depletion in rocket plumes, *Nature*, *390*, 62–65, doi:10.1038/36318.

SBSP Study Group. (2007), Space-based solar power as an opportunity for strategic security, *Tech. Rep. Director*, National Security Space Office Interim Assessment, Washington D. C. [Available at http://www.nss.org/settlement/ssp/library/final-sbsp-interim-assessment-release-01.pdf]

Siskind, D. E., M. H. Stevens, M. E. Hervig, and C. E. Randall (2013), Recent observations of high mass density polar mesospheric clouds: A link to space traffic? *Geophys. Res. Lett.*, *40*, 2813–2817, doi:10.1002/grl.50540.

Stenke, A., and V. Grewe (2005), Simulations of stratospheric water vapor trends: Impact on stratospheric ozone chemistry, *Atmos. Chem. Phys.*, *5*, 1257–1272.

Swain, M. R., M. N. Swain, A. Leisz, and R. R. Adt (1990), Hydrogen peroxide emissions from a hydrogen fueled engine, *Int. J. Hydrog. Energy*, *15*, 263–266.

Thomas, G. E., and J. Olivero (2001), Noctilucent clouds as possible indicators of global change in the mesosphere, *Adv. Space Res.*, *28*, 937–946.

Tian, W., M. P. Chipperfield, and D. Lu (2009), Impact of increasing stratospheric water vapor on ozone depletion and temperature change, *Adv. Atmos. Sci.*, *26*, 423–437.

van Vuuren, D. P., J. Edmonds, M. Kimono, K. Riahi, A. Thomson, K. Hibbard, G. C. Hurtt, T. Kram, V. Krey, and J.-F. Lamarque (2011), The representative concentration pathways: an overview, *Clim. Change*, *109*, 5, doi:10.1007/s10584-011-0148-z.

Vogel, B., T. Feck, and J.-U. GrooB (2011), Impact of stratospheric water vapor enhancements caused by CH4 and H2O increase on polar ozone loss, *J. Geophys. Res.*, *116*, D05301, doi:10.1029/2010JD014234.

Zeldovich, Y. B., P. Y. Sadonikov, and D. A. Frank-Kamenetskii. (1947), Oxidation of Nitrogen in Combustion (M. Shelef, Transl.), Academy of Sciences of USSR, Institute of Chemical Physics, Moscow, Russia.